Contents lists available at ScienceDirect

Journal of the Taiwan Institute of Chemical Engineers

Facile synthesis of zeolite NaX using rice husk ash without pretreatment

Phuong Lan Tran-Nguyen[a,*], Kim-Phung Ly[b], Luong Huynh Vu Thanh[b],
Artik Elisa Angkawijaya[c], Shella Permatasari Santoso[d], Nguyen-Phuong-Dung Tran[e],
Meng-Lin Tsai[e], Yi-Hsu Ju[c,f]

[a] Department of Mechanical Engineering, Can Tho University, Campus II, 3/2 street, Can Tho city 900100, Vietnam
[b] Department of Chemical Engineering, Can Tho University, Campus II, 3/2 street, Can Tho city 900100, Vietnam
[c] Graduate Institute of Applied Science and Technology, National Taiwan University of Science and Technology, #43, Sec. 4, Keelung Rd., Taipei 10607, Taiwan
[d] Department of Chemical Engineering, Widya Mandala Surabaya Catholic University, Kalijudan 37, Surabaya 60133, Indonesia
[e] Department of Materials Science and Engineering, National Taiwan University of Science and Technology, #43, Sec. 4, Keelung Rd., Taipei 10607, Taiwan
[f] Department of Chemical Engineering, National Taiwan University of Science and Technology, 43 Keelung Rd. Sec. 4, Taipei 10607, Taiwan

ARTICLE INFO

ABSTRACT

Rice husk ash (RHA) is an abundant agricultural waste in Mekong Delta, Vietnam. The utilization of RHA for zeolites production has been widely studied by pretreating RHA before reaction. In this study, zeolite NaX was synthesized directly using RHA without any pretreatment. Key parameters including molar ratios of SiO_2 to Al_2O_3 and Na_2O to Al_2O_3, reaction time, and aging time were investigated. The results showed that the optimal conditions for the synthesis of zeolite NaX are: molar ratio of SiO_2/Al_2O_3 = 4, molar ratio of Na_2O/Al_2O_3 = 10, reaction time = 4 h, and without aging. Zeolite NaX with a specific surface area of 388 m^2/g and a pore diameter of 12.37 Å was obtained, which were comparable to the published data. The method developed in this work is an energy and time saving, integrated, and environmental friendly process. It has the potential to be applied for synthesizing other types of zeolite.

1. Introduction

Zeolites are inorganic materials with regular microporous structure which have been widely developed and used in many applications [1,2]. The structure of zeolite consists of the network of tetrahedral $[SiO_4]^{4-}$ and $[AlO_4]^{5-}$ [1]. These tetrahedrons are linked through oxygen-spherical bonds to form an open structure with empty holes [2]. Many types of zeolite such as zeolite X, A, P1, Y or ZSM-5 have been successfully synthesized from commercial silica sources or wastes with high silica content [1,3−6]. Zeolite X which belongs to the faujasite (FAU) family with large pore size (about 8 Å) [1] possessed special properties in the adsorption of heavy metals, gas or organic wastes [1,7−8]. Zeolite X has been synthesized using silica sources such as kaolin [2], bauxite [1], diatomite [9], bagasse fly ash [10], coal fly ash [11], and RHA [4,12].

RHA, an agricultural waste, can cause serious environmental pollution [13]. Mekong Delta is the major agricultural center of Vietnam which produces tens of million ton of rice annually [14]. Rice husks are often used as fuel, partially replacing coal and gas [13]. A small portion of RHA, the residue of burning rice husk, is used as organic fertilizer, light concrete, or activated carbon [15]. However,

the amount of rice husk is huge and the main treatment is usually burning or landfilling [13]. These treatment methods cause greenhouse gas emissions, air pollution, and consume large areas for landfilling [13]. Meanwhile, RHA is well-known as a rich source of silica (about 90%) [16] and is an excellent source for the synthesis of zeolite, silica and cordierite [4,17,18]. Zeolite synthesis from RHA [11,13] opens a new route in alleviating environmental pollution caused by RHA.

In previous studies for producing zeolite NaX, RHA required calcination or chemical pretreatment before reaction [4,12,19]. Meanwhile, the processes involved were complicate, energy and time comsuming and low economic efficiency [4,5,12,20]. There were some reports on the synthesis of zeolite NaX using untreated RHA but the reaction time required was quite long [21,22]. In addition, previous studies have not given the full evaluation on the important factors that affected the synthesis of zeolite NaX from the RHA without calcination. In this study, the effects molar ratios of SiO_2/Al_2O_3 and Na_2O/Al_2O_3, reaction time and aging time on the final zeolite product were carefully investigated under mild conditions and shorter reaction time. The mechanism of the formation of NaX was also proposed. RHA and zeolite products were characterized by X-ray diffraction (XRD), field emission scanning electron microscopy (FESEM), dynamic light scattering (DLS), Brunauer - Emmett - Teller (BET), and X-ray fluorescence (XRF).

* Corresponding author.
E-mail address: tnplan@ctu.edu.vn (P.L. Tran-Nguyen).

2. Experimental

2.1. Raw materials

RHA was collected from Nam Tien Joint Stock Company, Tra Noc Industrial Park, Can Tho City, Vietnam. The collected ash was directly used for the zeolite synthesis. Other chemicals such as sodium hydroxide pellets and aluminum powder (purity 99%, Union Chemical Industry Company Ltd.) were obtained from commercial sources.

2.2. Synthesis of zeolite NaX

The synthesis procedure of zeolite NaX, based on previous studies with some modifications, is depicted in Fig. 1 [2,22]. RHA and NaOH solution (5 M) were placed in a round bottom flask and stirred at 300 rpm and 90°C for 3 h with a certain solid/liquid ratio [23]. A refluxed condenser was applied during the reaction. After the reaction, the products were collected and filtered to separate the aqueous fraction, mainly sodium silicate, from the solid fraction. $NaAlO_2$ solution was prepared by dissolving aluminum powder in NaOH solution according to the required molar ratio. Then, the prepared $NaAlO_2$ solution was gradually added to the aqueous fraction at 50°C and vigorously stirred for 2 h. After obtaining a homogeneous gel mixture, the mixture was heated to 90°C and kept for certain time T_1 (h). Then, the supernatant was aged at T_2 (h). The precipitate was then collected by filtration, centrifuged and dried at 100°C until constant weight to obtain the zeolite NaX powder. Each data was the results of triplicate experiments.

2.3. Characterization

The zeolite NaX products were characterized by using XRD, BET, FE-SEM, DLS and XRF while the composition of RHA was analyzed by using XRF and TGA. XRD was performed on a D8 Advance instrument (Bruker), with an X-ray diffractometer using CuK radiation (λ = 1.54056 Å) scanned at 7.0000 degree/min, an applied current of 30 mA and an accelerating voltage of 40 kV. FE-SEM measurement was taken with a Hitachi S-4800 scanning electron microscope. DLS from SZ-100 (Horiba) was used to determine the size distribution profile of NaX. The analysis of major and trace elements in RHA and the synthesized NaX was processed by using XRF (S8 TIGER Series 2, Bruker). TGA was also performed by using a thermogravimetric analyzer (Pyris Diamond TG-DTA, PerkinElmer Instrument, USA). BET was applied for determining the specific surface area and the pore diameter of the synthesized NaX. The sample was dried for 16 h at 105°C before being analyzed with a Nova 2000 (Quantachrome Instruments, USA).

3. Results and discussion

XRD was used to determine the polymorphism of SiO_2 in the untreated RHA [5]. Fig. 2a shows that only a broad peak of SiO_2 appeared at 2θ = 22°, indicating amorphous form of silica [5]. The amorphous SiO_2 dominated in the untreated RHA, so it was a potential material for zeolite synthesis [15]. Moreover, XRF result showed that silica accounts for > 95% of the RHA (Table 1). The total weight loss from room temperature to 800°C was about 1.5% (Fig. 2b). Very
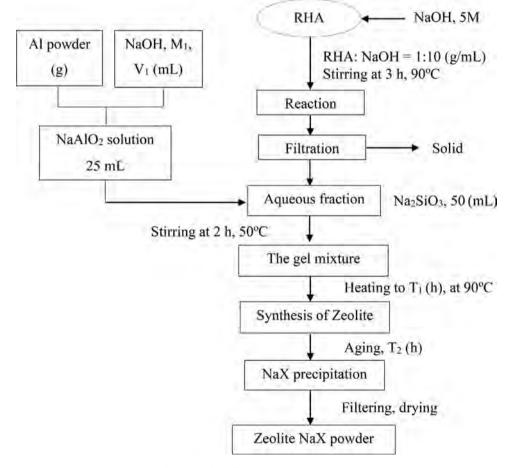

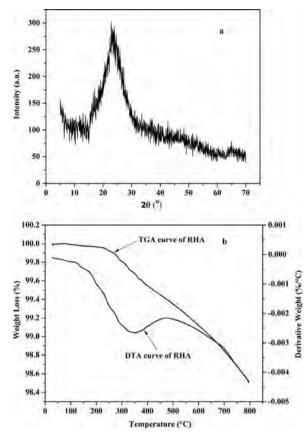**Fig. 1.** Flowchart of zeolite NaX synthesis process.

Fig. 2. XRD pattern of silica from RHA and thermogravimetric curve of RHA.
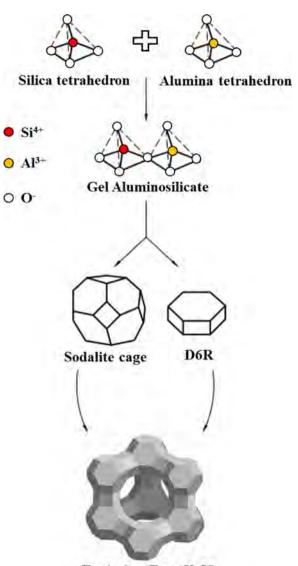
Table 1
Chemical composition of RHA used in this study.

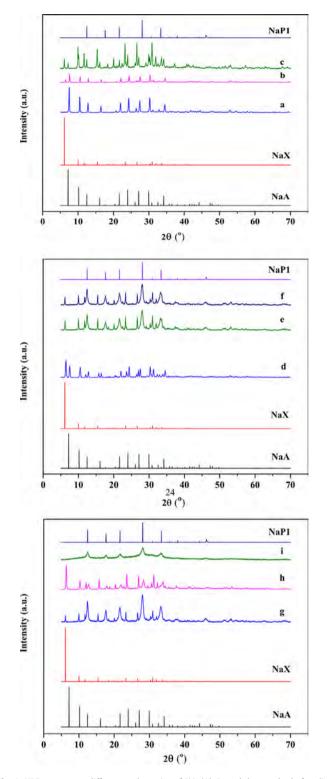| Elements	Content (%)
SiO_2	96.11
K_2O	1.47
Al_2O_3	1.16
CaO	0.48
P_2O_5	0.2
MnO	0.19
Fe_2O_3	0.15
Na_2O	0.11
SO_3	0.03
Sb_2O_3	0.03
CdO	0.02
SnO_2	0.02
ZnO	0.02
BaO	0.01
SrO	0.01
Ta_2O_5	0.01

Fig. 3. The proposed mechanism of zeolite NaX formation.

seeds, which enter the growth phase influenced by reaction time and temperature. Finally, the complete crystals of zeolite X are found.

3.1. Effect of SiO_2/Al_2O_3

Zeolites were synthesized at SiO_2/Al_2O_3 molar ratios from 2.0 to 4.5 with the other reaction conditions fixed (Fig. 4). The main peaks in XRD patterns of the synthesized zeolite were compared with the standard peaks of NaA, NaX and NAP1 (JCPDS card No. 38-0237, JCPDS card No. 43-0142 and JCPDS card No. 39-0219, respectively). In Fig. 4a, a single phase zeolite NaA was formed at SiO_2/Al_2O_3 = 2.0. When this ratio was increased to 2.5 (Fig. 4b), all peaks of zeolite NaA decreased and peaks of zeolite NaX appeared with low intensity. Al-Jubouri et al. successfully synthesized pure zeolite NaA at SiO_2/Al_2O_3 between 1.0 and 2.0 and obtained formation of zeolite X at a ratio > 2.0 [32]. In fact, as this ratio was increased from 3.0 to 4.0 (Fig. 4c-4h), a significant increase of zeolite NaX peaks intensity and decrease peaks intensity of zeolite NaA, which completely disappeared at a ratio of 4.0.

At ratios of 3.0 and 3.125, alternating formation of zeolite NaA and NaX was observed. More zeolite NaA was formed at a ratio of 3.0 while the main peak of zeolite NaX was found at a ratio of 3.125 with the coexistence of zeolite NaA. This result agrees with those reported in

little weight loss between 100 and 200°C was observed due to the removal of adsorbed water on the surface of particles. Some organic matter may be retained in RHA [24]. From 200 to 600°C, a more rapid weight loss was observed owing to decomposition of organic matter which was also reported by Fernandes et al. [25].

It was reported that 90°C is the suitable reaction temperature for zeolite X synthesis [2,12,26–29], so 90°C was used in this study. To better understand the formation of zeolite X [30,31], a reaction mechanism was proposed in Fig. 3. The mechanism could be described as follows: the precursor sources are firstly dissolved to form silica and alumina tetrahedra. The two tetrahedral are combined to form gel aluminosilicate, followed by formation of secondary structures such as sodalite cages and double six member-rings (D6R) in the presence of OH^-. The secondary structures then combine to create crystal

Fig. 4. XRD patterns at different molar ratios of SiO_2/Al_2O_3 and the standard of zeolite NaA, NaX and NaP1. (a) 2.0, (b) 2.5, (c) 3.0, (d) 3.125, (e) 3.25, (f) 3.5, (g) 3.75, (h) 4.0, and (i) 4.5.

literature when the ratio used was above 2.5 [28,33,34]. An increase of this ratio resulted in a decrease of NaA and the appearance of NaX [28]. Between the ratio of 3.25 - 4.0, the peak of NaA almost completely disappeared because the significant decrease in the solubility of Si^{4+} ions as Al^{3+} ion concentration was increased. The low concentrations of Si^{4+} ions favored the formation of structure such as double four member-ring (D4R); thus, zeolite A usually appeared at low SiO_2/Al_2O_3

ratio [4,28]. It was reported that SiO_2/Al_2O_3 ratio for the synthesis of zeolite NaA should be < 3.0 [32,35]. Alternating peaks of zeolite NaX and NaP1 were observed at a ratio of 3.25 and NaX with high intensity can be found at ratio > 3.5. Besides the predominant formation of zeolite NaX, the sample still contained a little zeolite NaP1. Similar results of NaX at a ratio of 4.0 using different feedstock were reported [3,36]. The tendency to form zeolite NaP1 when increasing this ratio was also mentioned previously [29,37]. At a ratio of 4.3, NaX was the dominant zeolite [37]. At ratio between 3.0 and 4.8, the products contained NaA, NaX and NaP1 [38].

As SiO_2/Al_2O_3 ratio was increased to 4.5 (Fig. 4i), zeolite NaP1 peaks started to appear. Similar trend was reported by Hildebrando et al. (2014) [39]. The formation of NaP1 was more significant when changing this molar ratio and a decrease of Al used favored the formation of zeolite NaP1 [36,40]. The control of the SiO_2/Al_2O_3 molar ratio was crucial to achieve single-phase zeolite NaX. A ratio of 4.0 was chosen to achive NaX zeolite crystallized with high intensity.

3.2. Effect of Na_2O/Al_2O_3

Previous studies reported different results in the synthesis of zeolite X when changing Na_2O/Al_2O_3 ratio [33,41,42]. In this study, Na_2O/Al_2O_3 ratios from 2.0 to 12 were investigated (Fig. 5). At a ratio of 2.0, only amorphous phase was found. When this ratio was increased to 8.0, the peaks of zeolite NaX and NaP1 appeared with NaX as the dominant phase. To eliminate zeolite NaP1, $Na_2O/$
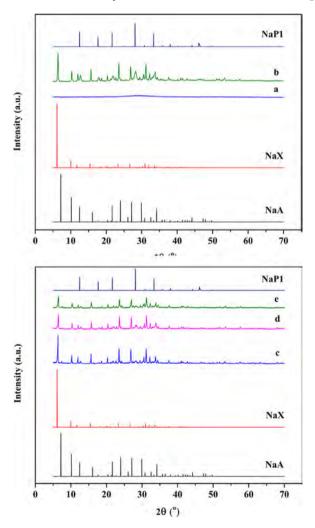

Fig. 5. XRD patterns at different molar ratios of Na_2O/Al_2O_3 and the standard of zeolite NaA, NaX and NaP1. (a) 2.0, (b) 8.0, (c) 10.0, (d) 11.0, and (e) 12.0.

Al$_2$O$_3$ = 12.0 was applied based on previous studies which reported that an increase of alkalinity of the reaction mixture inhibited zeolite NaP1 formation [3,34,43]. However, more alkaline added resulted in a decrease of peaks intensity of zeolite NaX (Fig. 5e). An increase of NaOH would decrease NaX owing to poor stability of zeolite in high alkaline solution [42]. Fig. 5d shows similar crystallization to that of Na$_2$O/Al$_2$O$_3$ = 12 and the peaks of zeolite NaX were weaker than that of Na$_2$O/Al$_2$O$_3$ = 8.0. The characteristic peaks of zeolite NaX indicated high crystallinity at a ratio of 10.0 (Fig. 5c). Crystalize zeolite NaX only existed with high intensity when optimal alkalinity of the reaction mixture was employed [44].

OH$^-$ group was the stimulator in forming primary structures and helped forming the bonds between the SiO$_4$ and AlO$_4^-$ tetrahedra. If alkalinity of the mixture was low, the OH$^-$ group was not enough to form bonds of tetrahedra. When the alkaline concentration reached the required level, tetrahedral bonds were easily formed to facilitate the crystallization of zeolite X. At too high alkalinity, the tetrahedra would be partially dissolved, resulting in a decrease of the crystallinity [45]. At Na$_2$O/Al$_2$O$_3$ = 10.0, the product was of high crystallinity intensity with almost no interference.

3.3. Effect of reaction time

Fig. 6 shows the effect of reaction time on the synthesis of zeolite NaX. At 2 h, the characteristic peaks of zeolite NaX appeared with low intensity. The optimal reaction time with high crystallinity was between 3 and 6 h [28]. In this study, a reaction time of 4 h was employed to obtain NaX with high crystallinity (Fig. 6b).

A decrease in characteristic peaks intensity of zeolite NaX and the formation of zeolite NaP1 with low intensity were observed at 6 h. At prolonged reaction time, the peak intensity of the desired products started to decrease [46]. Only zeolite NaX crystallized well at a specific reaction time [9,47]. At 8 h, the result was not much different from that of 6 h. However, when the reaction time was increased from 4 h to 6 h, crystallization intensity rapidly increased and formed relatively uniform crystals [48]. This trend was also mentioned before [28,49].
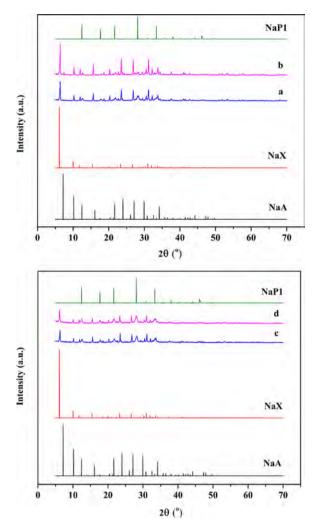
Fig. 7 indicates that the crystals were not uniformly formed and some non-crystallized aluminosilicate gel regions existed at 2 h. At 4 h, the crystals formed complete structure with almost no visible amorphous region. The morphology of NaX crystals in this work was similar to those of Garcia et al. (2016) and Zhang et al.(2019) [36,50]. Zeolite X had higher crystallinity at 4 h than that at longer time in other studies using RHA [4,12]. Microwave assistance and ultrasonic treatment could be used to speed up dissolution of precursors, help formation of bonds, and promote rapid growth of crystals [27,51].

The effect of aging time on the nucleation and crystallization of zeolite crystal was reported before [34,52], and investigated in this study. Fig. 8 shows that aging time from 0 to 24 h had no effect. This can be explained because the prolonged aging time would support the formation of GIS family zeolites like zeolite P insteacd of zeolite A and X. Similar results were reported by Ghasemi and Younesi (2012) and Thuadaij and Nuntiya (2012) [19,53]

In this work, the alkalinity of solution was investigated because it also affected on the nucleation and crystallization of zeolite crystals. In stead of using microwave and ultrasound assistance to help shortening nucleation and reaction time of zeolite [27,51], this study employed the increase of solution alkalinity to improve the reaction rate. The morphology of samples obtained at aging time of 0 h and 6 h was examined (Fig. 8). No significant difference between 0 h and 6 h was observed; thus, aging was unnecessary in this work.

3.4. Comparison of the current method with published methods

Many different feedstocks were used for zeolite synthesis such as commercial/natural mineral sources, wastes from industrial and agricultural production such as diatomite, fly ash and RHA. Generally,

Fig. 6 . XRD patterns at different reaction time and the standard of zeolite NaA, NaX and NaP1. (a) 2 h, (b) 4 h, (c) 6 h, and (d) 8 h.

when using waste and natural mineral precursors, most required pretreatment like fusing at high temperatures or extracting silica which needs long time before subjecting to zeolite synthesis. Thuadaij et al. (2012) prepared zeolite X from fly ash and amorphous silica RHA by fusion at 550°C [53] while Muriithi et al. (2020) used fly ash as the precursor with a reaction time of 9 h [11]. Wang et al. (2018) carried out the synthesis in 24 h to extract Na$_2$SiO$_3$ from RHA [20]. Ghasemi and Younesi pretreated (2012) RHA with HCl, then calcinated at 700°C for 6 h before proceeded to the synthesis of zeolite X [19]. The surface area (m^2/g) and pore diameter (Å) of their synthesized NaX was 89.96 and 92, respectively compared to a surface area of 388.4 and a pore volume of 12.37 of this study. In terms of reaction time, this study required is much shorter (4 h) than the 48 h required in their study [19]. The research of Katsuki et al. (2009) used a procedure similar to this study, and obtained NaX zeolite with a surface area of 553 m^2/g at a longer reaction time of 6 h. However, rice husk had to be burned in nitrogen gas at 600-1000°C before used as the raw material for the synthesis [22]. Although Zhang et al. (2013) synthesized NaX using commercial silica source and a specific surface area of 526 m^2/g was obtained; however, the reaction time needed was 15 h [26], which was much longer than that of this work (4 h).

This study could directly synthesize zeolite X using RHA without calcination and the optimal conditions were SiO$_2$/Al$_2$O$_3$ molar ratio of 4.0, Na$_2$O/Al$_2$O$_3$ molar ratio of 10.0, reaction time of 4 h and without aging. The ratio of SiO$_2$/Al$_2$O$_3$ of 4 was comparable with that from other publications; nevertheless, the Na$_2$O/Al$_2$O$_3$ molar ratio of 10
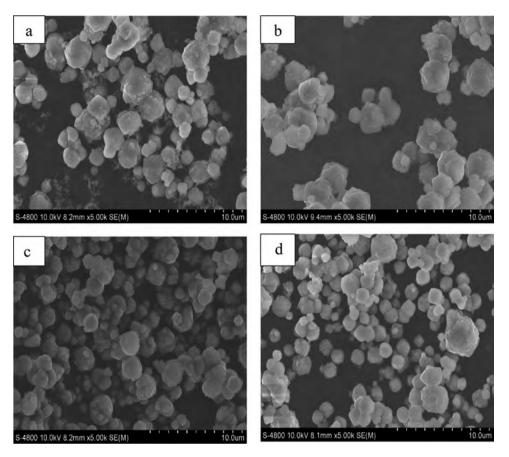
Fig. 7. FESEM images of the NaX at different reaction time. (a) 2 h, (b) 4 h, (c) 6 h, and (d) 8 h.

was much higher than that of other studies. The higher molar ratio of Na_2O/Al_2O_3 would help the formation of high purity and crystallinity NaX as mentioned. Although this study used agricultural by-product as the feedstock, the specific surface area of the synthesized NaX was quite high (388 m^2/g). Additionally, DLS result showed that the average particles size of the synthesized NaX was 484.1 nm.

The total reaction time, including extraction of silica, stirring to obtain homogenous mixture and synthesis of zeolite, was estimated to be about 10 h while calcination or fusion was not required, thus the process was carried out at mild conditions. Therefore, this work could provide an integrated and promising process to obtain valuable materials with low energy consumption and low cost. The low pore diameter of the synthesized NaX (12.37 Å) was due to the use of RHA

without calcination. This precursor source may contain organic matters which partially blocked the pores of the products, resulting in lower specific surface area and pore diameter of NaX than those of some studies, as shown in Table 2.

In general, this study was performed to evaluate the impact of factors affecting the formation of zeolite NaX from RHA without pretreatment. The final product was the highly crystallized zeolite NaX with a relatively large surface area compared to similar studies using other waste sources. Materials with a large surface area have been mentioned in previous studies with good adsorption capacity of CO_2, or dyes [9,13,54,55]. Our preliminary results on the adsorption of methylene blue by zeolite NaX showed that the removal capacity of the dye can be more than 80% (data not shown). In addition, the

Table 2
Comparison of zeolite synthesized in this study with those in other studies.

Raw materials	Reaction conditions				Surface area (m^2/g)	Pore diameter (Å)	References
	Ratio of SiO_2/Al_2O_3	Ratio of Na_2O/Al_2O_3	Reaction time (h)	Aging time (h)			
SiO_2 commercial	3.5	3.5	15	-	526	-	[26]
Diatomite	-	-	5	0.5	53	-	[9]
Fly ash and amorphous silica[a] (Fused 550°C − 1 h)	3.71	-	24	18[b]	232.73	-	[53]
Coal fly ash (Fused 550°C − 1.5 h with NaOH)	3.63	4.9	9	0	257	122	[11]
RHA (extracted Na_2SiO_3 by NaOH in 70°C and 24 h)	4.0	5.5	24	0	644	18.8	[20]
RHA (pretreated HCl and calcined at 700°C in 6 h)	4.0	-	48	0	89.96	92	[19]
Rice husk (carbonized at 600-1000°C for 1h and extracted Na_2SiO_3 by NaOH 2N at 90°C)	1.9	-	6	0	553	-	[22]
RHA (without calcined)	4.0	10.0	4	0	388.41	12.37	This study

[a] silica was extracted from RHA
[b] aging before reaction

[17] Kaviyarasu K, Manikandan E, Kennedy J, Jayachandran M, Maaza M. Rice husks as a sustainable source of high quality nanostructured silica for high performance Li-ion battery requital by sol-gel method − a review. Adv Mater Lett 2016;7: 684–96.

[18] Sembiring S, Simanjuntak W, Situmeang R, Riyanto A, Sebayang K. Preparation of refractory cordierite using amorphous rice husk silica for thermal insulation purposes. Ceram Int 2016;42:8431–7.

[19] Ghasemi Z, Younesi H. Preparation of free-template nanometer-sized Na−A and−X zeolites from rice husk ash. Waste Biomass Valorization 2012;3:61–74.

[20] Wang Y, Du T, Jia H, Qiu Z, Song Y. Synthesis, characterization and CO_2 adsorption of NaA, NaX and NaZSM-5 from rice husk ash. Solid State Sci 2018;86:24–33.

[21] Kurniawan W, Hinode H. Lean condition procedure for utilization of silica from rice husk as zeolite precursor. Indonesian J Comput, Eng Des 2020;2:111–21.

[22] Katsuki H, Komarneni S. Synthesis of Na-A and/or Na-X zeolite/porous carbon composites from carbonized rice husk. J Solid State Chem 2009;182:1749–53.

[23] Shelke VR, Bhagade SS, Mandavgane SA. Mesoporous silica from rice husk ash. Bull Chem React Eng Catal 2010;5:63–7.

[24] Thiedeitz M, Schmidt W, Harder M, Krankel T. Performance of rice husk ash as supplementary cementitious material after production in the field and in the lab. Materials 2020;13:4319.

[25] Fernandes IJ, Calheiro D, Kieling AG, Moraes CAM, Rocha TLAC, Brehm FA, Modolo RCE. Characterization of rice husk ash produced using different biomass combustion techniques for energy. Fuel 2016;165:351–9.

[26] Zhang X, Tang D, Zhang M, Yang R. Synthesis of NaX zeolite: Influence of crystallization time, temperature and batch molar ratio SiO_2/Al_2O_3 on the particulate properties of zeolite crystals. Powder Technol 2013;235:322–8.

[27] Ansari M, Aroujalian A, Raisi A, Dabir B, Fathizadeh M. Preparation and characterization of nano-NaX zeolite by microwave assisted hydrothermal method. Adv Powder Technol 2014;25:722–7.

[28] Yang T, Han C, Liu H, Yang L, Liu D, Tang J, Luo Y. Synthesis of Na-X zeolite from low aluminum coal fly ash: characterization and high efficient As (V) removal. Adv Powder Technol 2019;30:199–206.

[29] Nazir LSM, Yeong YF, Sabdin S. Formation of pure NaX zeolite: effect of ageing and hydrothermal synthesis parameters. IOP Conf Ser: Mater Sci Eng 2018;458:012002.

[30] Murayama N, Tanabe M, Yamamoto H, Shibata J. Reaction, mechanism and application of various zeolite syntheses from coal fly ash. Mater Trans 2003;44:2475–80.

[31] Masoudian SK, Sadighi S, Abbasi A. Synthesis and characterization of high aluminum zeolite X from technical grade materials. Bull Chem React Eng 2013;8:54–60.

[32] Al-Jubouri SM, Sabbar HA, Lafta HA, Waisi BI. Effect of synthesis parameters on the formation 4A zeolite crystals: characterization analysis and heavy metals uptake performance study for water treatment. Desalin Water Treat 2019;165:290–300.

[33] Garshasbi V, Jahangiri M, Anbia M. Equilibrium CO_2 adsorption on zeolite 13X prepared from natural clays. Appl Surf Sci 2017;393:225–33.

[34] Abdullahi T, Harun Z, Othman MHD. A review on sustainable synthesis of zeolite from kaolinite resources via hydrothermal process. Adv Powder Technol 2017;28:1827–40.

[35] Ayele L, Pérez-Pariente J, Chebude Y, Díaz I. Conventional versus alkali fusion synthesis of zeolite A from low grade kaolin. Appl Clay Sci 2016;32:485–90.

[36] García A, López CM, García LV, Casanova J, Goldwasser M. Improvements in the synthesis of zeolites with low Si/Al ratio from Venezuelan sodium silicate for an environmentally friendly process. Ing e Investig 2016;36:62–9.

[37] Zhou C, Alshameri A, Yan C, Qiu X, Wang H, Ma Y. Characteristics and evaluation of synthetic 13X zeolite from Yunnan's natural halloysite. J Porous Mater 2013;20:587–94.

[38] Wang C, Zhou J, Wang Y, Yang M, Li Y, Meng C. Synthesis of zeolite X from low-grade bauxite. J Chem Technol Biotechnol 2013;88:1350–7.

[39] Hildebrando EA, Andrade CGB, Rocha Junior CAFD, Angélica RS, Valenzuela-Diaz FR, Neves RdDF. Synthesis and characterization of zeolite NaP using kaolin waste as a source of silicon and aluminum. Mater Res 2014;17:174–9.

[40] Ali IO, El-Sheikh SM, Salama TM, Bakr MF, Fodial MH. Controllable synthesis of NaP zeolite and its application in calcium adsorption. Sci China Mater 2015;58:621–33.

[41] Juengsuwattananon K, Winnefeld F, Chindaprasirt P, Pimraksa K. Correlation between initial SiO_2/Al_2O_3, Na_2O/Al_2O_3, Na_2O/SiO_2 and H_2O/Na_2O ratios on phase and microstructure of reaction products of metakaolin-rice husk ash geopolymer. Constr Build Mater 2019;226:406–17.

[42] Nazir LSM, Yeong YF, Chew TL. Controlled growth of Faujasite Zeolite with NaX topology by manipulating solution aging and Na_2O/Al_2O_3 ratios. Colloid Surf A-Physicochem Eng Asp 2020;600:124803.

[43] Qiu X, Liu Y, Li D, Yan C. Preparation of NaP zeolite block from fly ash-based geopolymer via in situ hydrothermal method. J Porous Mater 2015;22:291–9.

[44] Chaves TF, Pastore HO, Cardoso D. A simple synthesis procedure to prepare nano-sized faujasite crystals. Microporous Mesoporous Mater 2012;161:67–75.

[45] Ngoc DT, Pham TH, Nguyen KDH. Synthesis, characterization and application of nanozeolite NaX from Vietnamese kaolin. Adv Nat Sci: Nanosci Nanotechnol 2013;4:1–12.

[46] Sivalingam S, Sen S. Swift sono-hydrothermal synthesis of pure NaX nanocrystals with improved sorption capacity from industrial resources. Appl Surf Sci 2019;463:190–6.

[47] Johnson E, Asik J, Arshad S. The effect of crystallization time and temperature on hydrothermal synthesis of zeolite Nax from Bongawan kaolin. FEIIC Int J Eng Technol 2016;13:33–9.

[48] Ferdov S. Conventional synthesis of layer-like zeolites with faujasite (FAU) structure and their pathway of crystallization. Microporous Mesoporous Mater 2020;303:110263.

[49] Grand J, Awala H, Mintova S. Mechanism of zeolites crystal growth: new findings and open questions. Cryst Eng Comm 2016;18:650–64.

[50] Zhang S, Cui M, Chen J, Ding Z, Wang X, Mu Y, Meng C. Modification of synthetic zeolite X by thiourea and its adsorption for Cd (II). Mater Lett 2019;236:233–5.

[51] Ng TYS, Chew TL, Yeong YF, Jawad ZA, Ho CD. Zeolite RHO synthesis accelerated by ultrasonic irradiation treatment. Sci Rep 2019;9:1–11.

[52] Liu L, Du T, Li G, Yang F, Che S. Using one waste to tackle another: Preparation of a CO_2 capture material zeolite X from laterite residue and bauxite. J Hazard Mater 2014;278:551–8.

[53] Thuadaij P, Nuntiya A. Preparation and characterization of faujasite using fly ash and amorphous silica from rice husk ash. Procedia Eng 2012;32:1026–32.

[54] Hor KY, Chee JMC, Chong MN, Jin B, Saint C, Poh PE, Aryal R. Evaluation of physicochemical methods in enhancing the adsorption performance of natural zeolite as low-cost adsorbent of methylene blue dye from wastewater. J Clean Prod 2016:1–13.

[55] Krachuamram S, Chanapattharapol KC, Kamonsutthipaijit N. Synthesis and characterization of NaX-type zeolites prepared by different silica and alumina sources and their CO_2 adsorption properties. Microporous Mesoporous Mater 2020:310.

[56] Dehghani MH, Dehghan A, Alidadi H, Dolatabadi M, Mehrabpou M, Converti A. Removal of methylene blue dye from aqueous solutions by a new chitosan/zeolite composite from shrimp waste:. Kinetic Equil Study 2017; 34:1699–707.

[57] Abasiana P, Radmansourib M, Jouybaric MH, Ghasemid MV, Mohammadie A, Iranif M, et al. Incorporation of magnetic NaX zeolite/DOX into the PLA/chitosan nanofibers for sustained release of doxorubicin against carcinoma cells death in vitro. Int J Biol Macromol 2019;121:398–406.

[58] Cao J, Wang P, Shen J, Sun Q. Core-shell Fe_3O_4@zeolite NaA as an Adsorbent for Cu^{2+}. Materials 2020;13:5047.